

# Global Energy and Water Balances in the Latest Reanalyses

Suchul Kang<sup>1,2</sup> and Joong-Bae Ahn<sup>2</sup>

<sup>1</sup>APEC Climate Center (APCC), Busan, Korea

<sup>2</sup>Division of Earth Environmental System, Pusan National University, Busan, Korea

(Manuscript received 23 April 2015; accepted 31 August 2015)

© The Korean Meteorological Society and Springer 2015

**Abstract:** The recently released Japanese 55-year Reanalysis (JRA-55) data are evaluated and compared with three other global reanalyses, namely Interim version of the next European Centre for Medium-Range Weather Forecasts (ECMWF) Re-Analysis (ERA-Interim), Modern Era Retrospective-Analysis for Research and Applications (MERRA) and Climate Forecast System Reanalysis (CFSR), in terms of global energy and water balances. All four reanalyses show an energy imbalance at TOA and surface. Especially, clouds in JRA-55 are optically weaker than those in the three other reanalyses, leading to excessive outgoing longwave radiation, which in turn causes negative net energy flux at TOA. Moreover, JRA-55 has a negative imbalance at surface and at TOA, which is attributed to systematic positive biases in latent heat flux over the ocean. As for the global water balance, all reanalyses present a similar spatial pattern of the difference between evaporation and precipitation (E-P). However, JRA-55 has a relatively strong negative (positive) E-P in the Intertropical Convergence Zone and South Pacific Convergence Zone (extratropical regions) due to overestimated precipitation (evaporation), in spite of the global net being close to zero. In time series analysis, especially in E-P, significant stepwise changes occur in MERRA, CFSR and ERA-Interim due to the changes in the satellite observing system used in the data assimilation. Both MERRA and CFSR show a strong downward E-P shift in 1998, simultaneously with the start of the assimilation of AMSU-A sounding radiances. ERA-Interim exhibits an upward E-P shift in 1992 due to changes in observations from the SSM/I of new DMSP satellites. On the contrary, JRA-55 exhibits less trends and remains stable over time, which may be caused by newly available, homogenized observations and advances in data assimilation technique.

**Key words:** Energy balance, water balance, JRA-55, ERA-interim, MERRA, CFSR

## 1. Introduction

Reliable observational data are very useful in many respects, but are limited in the analysis of climate variation and past climate change because of their discontinuity and short history. Reanalysis has been proposed to overcome such observational limitations, with evenly distributed, long-term global atmospheric data being obtained. For producing global atmospheric

reanalysis datasets, a variety of observations (e.g., satellite instruments, weather stations, ships, buoys) is assimilated into a numerical model, allowing the spatial and temporal observational gaps to be filled in a manner consistent with the model physics and dynamics (Uppala et al., 2008).

Much of the effort in improving the qualities of globally gridded reanalyses has been devoted to increasing our comprehension of the energy and hydrological cycles (e.g., Trenberth et al., 2009; Stephens et al., 2012). Despite the greatly improved accuracy of atmospheric reanalyses, the global energy and water budgets generally remain imbalanced due to observational uncertainties and incomplete knowledge of the physical processes (Trenberth et al., 2009; Cullather and Bosilovich, 2012).

The energy balances at top of atmosphere (TOA) and at surface can be used as a diagnostic to examine the accuracy of the reanalyses. In other words, the reliability of the data can be assessed in terms of the degree of the balances of physical properties at the interfaces. Consequently, many studies (e.g., Trenberth et al., 2009, 2011; Cullather and Bosilovich, 2012) have compared the performances of reanalyses by focusing on the extent of energy and water balances.

The Japan Meteorological Agency (JMA) started production of the second Japanese global atmospheric reanalysis, called the Japanese 55-year Reanalysis (JRA-55), in 2010 (Ebita et al., 2011) and distribution of it in October 2013. According to the interim report (Ebita et al., 2011), JRA-55 is the first comprehensive reanalysis to cover the last half-century with higher resolution of T319 and the first one to adopt four-dimensional variational analysis (4D-Var) over the period. Kobayashi et al. (2015) insisted that JRA-55 was extensively improved compared to the previous reanalysis product of JMA, called the Japanese 25-year Reanalysis (JRA-25), in terms of the global net energy fluxes at TOA and at surface. However, few studies have compared the reliability of JRA-55 with other reanalyses in respect of energy and water budgets.

Apart from JRA-55, several institutes have recently produced and offered the new generation of global reanalyses with higher resolution finer than 1° by improving various factors such as observations, data assimilation method, and dynamical and physical processes. The interim version of the next European Centre for Medium-Range Weather Forecasts (ECMWF) Re-Analysis (ERA-Interim) (Dee et al., 2011), the

Corresponding Author: Joong-Bae Ahn, Department of Atmospheric Sciences, Pusan National University, 2, Busandaehak-ro, 63 beong-gil, Geumjeong-gu, Pusan 609735, Korea.  
E-mail: jbahn@pusan.ac.kr

**Table 1.** Main characteristics of the four reanalyses.

	ERA-Interim	MERRA	CFSR	JRA-55
Horizontal resolution	T255 (~78 km)	1/2 latitude x 2/3 longitude (~55 km)	T382 (~38 km)	TL319 (~55 km)
Vertical levels (top level)	60 levels (0.1 hPa)	72 levels (0.01 hPa)	64 levels (0.26 hPa)	60 levels (0.1 hPa)
Period	1979-present	1979-present	1979-present	1958-present
Assimilation scheme	4DVAR	3DVAR	3DVAR	4DVAR

Climate Forecast System Reanalysis (CFSR) (Saha et al., 2010) and the Modern Era Retrospective-Analysis for Research and Applications (MERRA) (Rienecker et al., 2011) are the latest global atmospheric reanalyses produced by the ECMWF, the National Centers for Environmental Prediction (NCEP) and the NASA's Global Modeling and Assimilation Office (GMAO), respectively. These data have been favorably evaluated as successful alternatives to the earlier versions of global atmospheric reanalyses (e.g., Hodges et al., 2011; Quadro et al., 2013). According to the analysis of Trenberth et al. (2011), these reanalyses markedly improved the representation of the hydrological cycle, although the energy and water budgets are not conserved.

In this study, the capability of JRA-55 is newly explored in light of global energy and water balances at surface and TOA by comparing with other new atmospheric reanalyses, such as ERA-Interim, CFSR and MERRA. The meteorological reanalyses used in the study are introduced in section 2 and their energy and water balances are illustrated in section 3. The summary and discussions are presented in section 4.

## 2. Data and methods

### a. Global reanalyses

In this study, four different global atmospheric retrospective analyses are used: JRA-55, ERA-interim, MERRA and CFSR. The main characteristics of the reanalyses are summarized in Table 1.

#### (1) JRA-55

JRA-55 has been produced by JMA's operational data assimilation system, and incorporates many improvements that have been achieved since JRA-25, such as the revised long-wave radiation scheme, four-dimensional variational analysis (4D-Var) and variational bias correction (VarBC) for satellite radiances (Kobayashi et al., 2015). The global spectral model of JRA-55 is based on Reduced Gaussian with TL319 (~55 km) and a hybrid sigma-pressure coordinate scheme utilizing 60 levels up to 0.1 hPa.

#### (2) ERA-Interim

ERA-Interim represents an undertaking by ECMWF to produce a reanalysis with an improved atmospheric model and assimilation system that replaces those used in ERA-40 (Dee et al., 2011). ERA-interim uses the Integrated Forecast System,

cycle 31R1 (IFS31R1) integrated at a T255 (~80 km) horizontal resolution with 60 vertical hybrid levels extending from the surface to 0.1 hPa. ERA-interim employs 4D-VAR with VarBC for satellite radiances.

#### (3) MERRA

MERRA produced by NASA uses the Goddard Earth Observing System Data Assimilation System, version 5 (GEOS-5) (Rienecker et al., 2008), at a resolution of 2/3° longitude by 1/2° latitude (~55 km) with 72 Lagrangian vertical levels extending from the surface to 0.01 hPa. The data assimilation uses three-dimensional variational data assimilation (3D-VAR) as the assimilation framework and the incremental analysis updates (IAU) procedure to slowly adjust the model state toward the observed state. As with all the reanalyses, observations are quality controlled and bias corrected before assimilation, including the satellite radiances. Additionally, rain rates from SSM/I and the Tropical Rainfall Measuring Mission (TRMM) satellites are assimilated.

#### (4) CFSR

CFSR is an NCEP reanalysis derived from a coupled atmosphere-ocean-land-sea ice system. The atmosphere resolution of CFSR is T382 (~38 km) with 64 hybrid vertical levels extending from the surface to 0.26 hPa. Its ocean resolution is ~1/2° with 40 levels to a depth of 4737 m. CFSR adopts 3D-VAR based on grid-point statistical interpolation (GSI), with flow dependence for background error variances (Saha et al., 2010; Rienecker et al., 2011). Variational quality control of observations is also included.

### b. Supplementary data

Radiation fluxes at surface and TOA are evaluated against satellite data, namely Clouds and the Earths Radiant Energy System (CERES)-Energy Balanced and Filled (EBAF) dataset edition 2.7 (Loeb et al., 2009). Precipitation data came from the newer version 2.2 of Global Precipitation Climatology Project (GPCP) data (Adler et al., 2003), which are derived from a mix of satellite estimates and in-situ rain gauge measurements. Latent heat fluxes over the ocean were obtained from the Woods Hole Oceanographic Institution (WHOI) Objectively Analyzed air-sea Heat Fluxes (OAFflux) dataset, which uses an optimal blending of multi-platform satellite retrievals, surface moorings, ship reports and global atmospheric reanalyses (Yu and Weller, 2007).

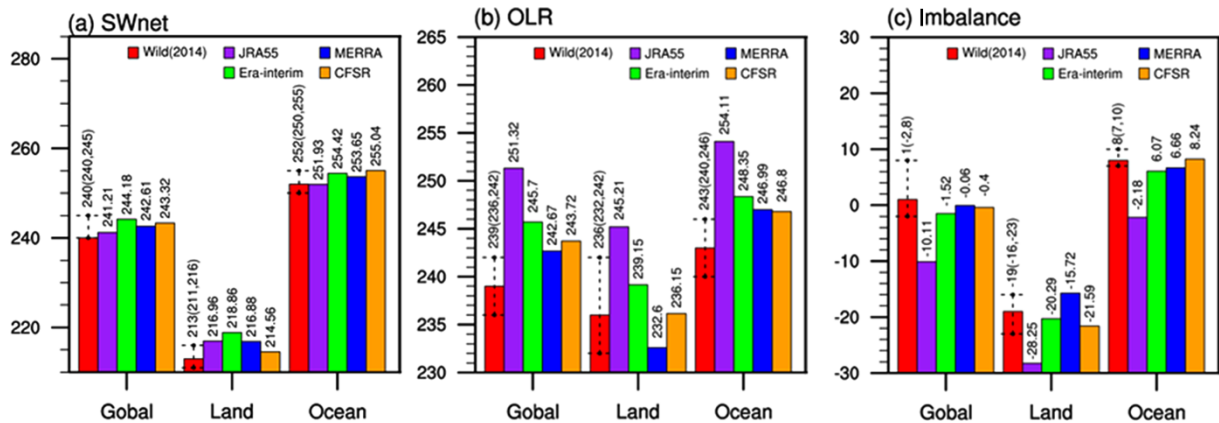


**Fig. 1.** Annual mean (a) net shortwave radiation (SWnet), (b) OLR and (c) energy imbalance at TOA for global, global land and global ocean ( $W m^{-2}$ ). Values from JRA-55, ERA-Interim, MERRA and CFSR are for the period 2001-2010, whereas those from Wild et al. (2014) represent present-day climate conditions at the beginning of the 21st century with their uncertainty ranges in brackets.

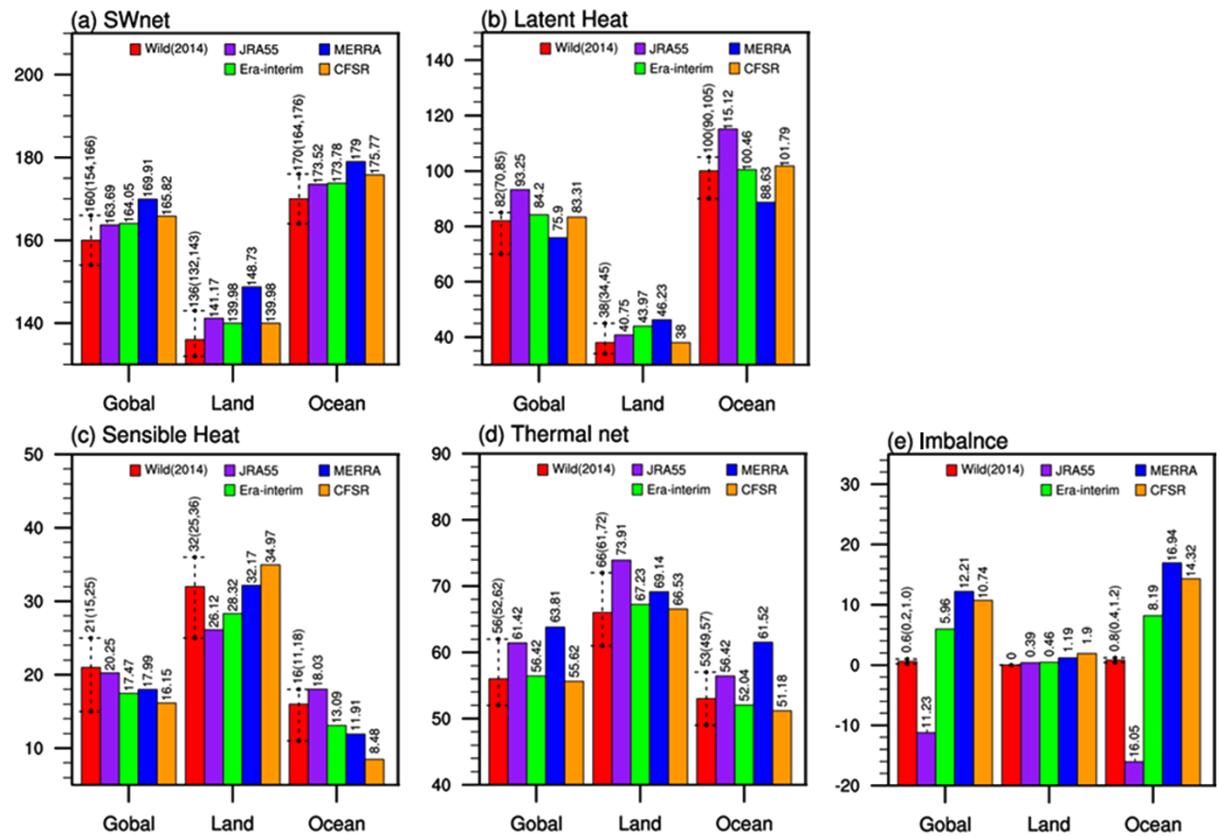


**Fig. 2.** Annual mean (a) net shortwave radiation (SWnet), (b) latent heat, (c) sensible heat, (d) net thermal radiation and (e) energy imbalance at surface for global, global land and global ocean ( $W m^{-2}$ ). Values from JRA-55, ERA-Interim, MERRA and CFSR are for the period 2001-2010, whereas those from Wild et al. (2014) represent present-day climate conditions at the beginning of the 21st century with their uncertainty ranges in brackets.

### 3. Results

#### a. Global mean climatology

Recently, Wild et al. (2014, hereafter Wild2014) newly esti-

mated the components of the globally averaged energy balance in addition to their uncertainty ranges using both observations and modeling results performed within the Coupled Model Intercomparison Project Phase 5 (CMIP5). Furthermore, they suggested best estimates for mean energy balance components

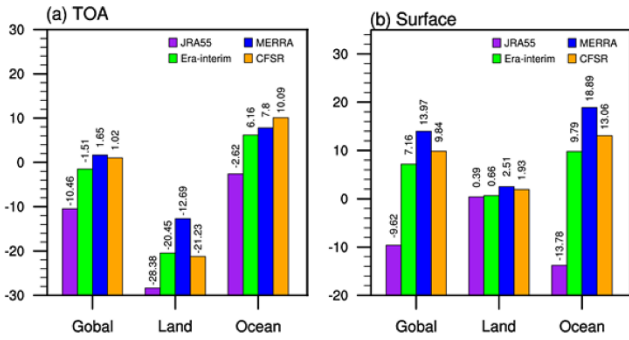


**Fig. 3.** Energy imbalances at the (a) TOA and (b) surface for global, global land and global ocean ( $W m^{-2}$ ). Values are derived from JRA-55, ERA-Interim, MERRA and CFSR for the 35-year base climate period of 1979-2013.

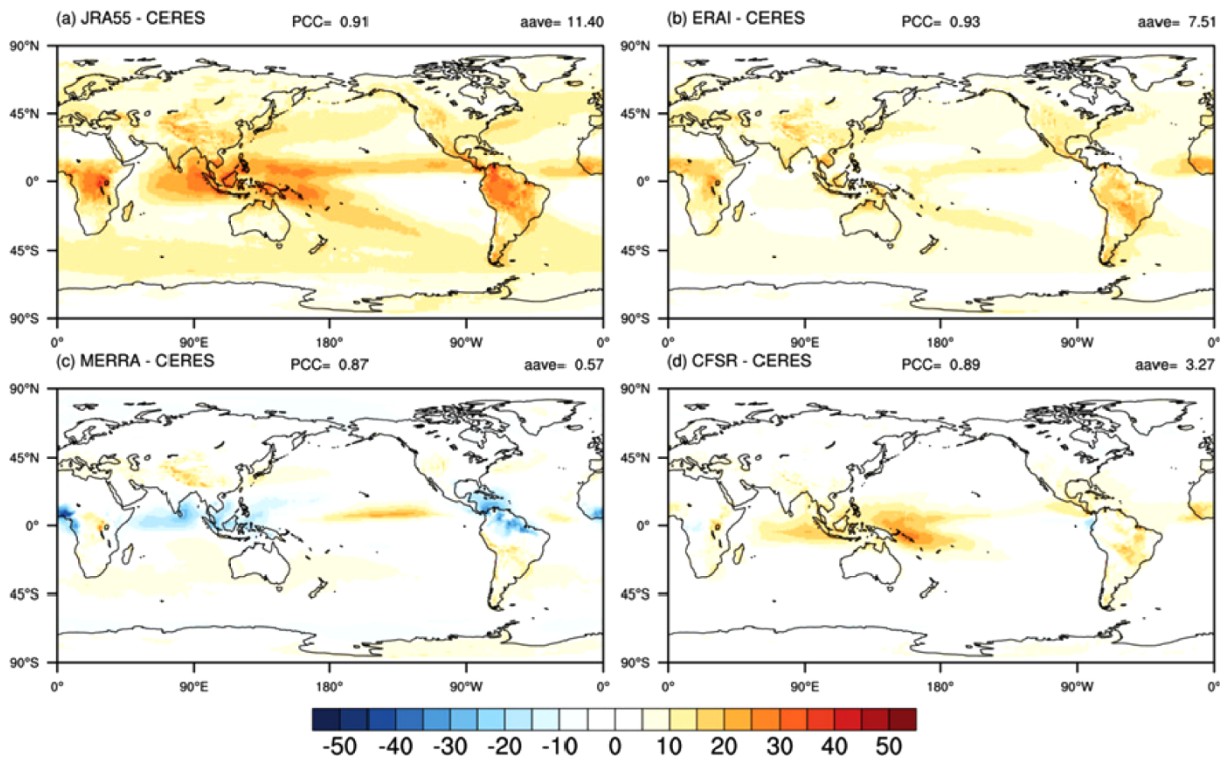
over the land and ocean separately. Here, the energy balances derived from reanalyses are evaluated by comparing with the estimates proposed by Wild2014.

Figure 1 shows the energy fluxes and their uncertainties at TOA derived from the four reanalyses and Wild2014. These data are averaged over 10 years from 2001 to 2010, the same analysis period as Wild2014. Net shortwave radiations in the four reanalyses are mostly within the uncertainty ranges of Wild2014, while the outgoing longwave radiation (OLR), especially in JRA-55, is larger than the Wild2014. Since OLR

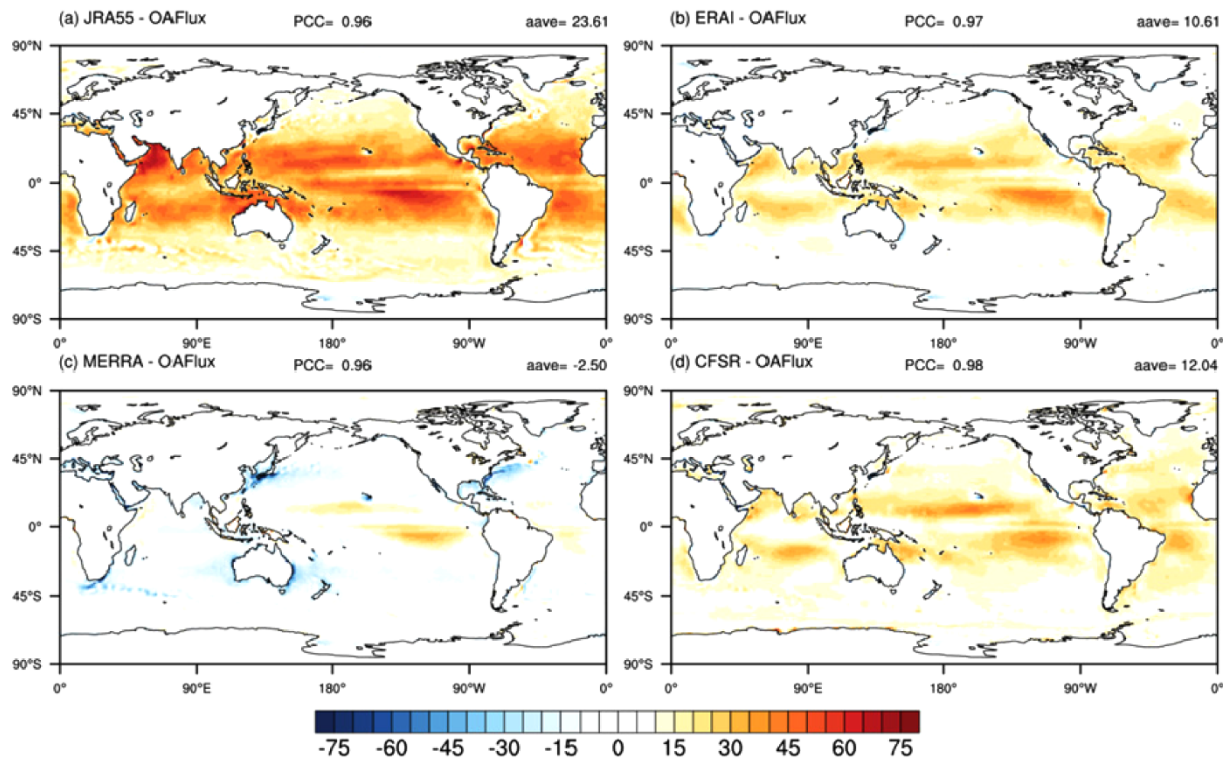
is generally affected by clouds in the atmosphere, the large OLR value in the reanalyses can be interpreted as optically thin clouds. That is, the weaker effect of clouds may induce the increased OLR in JRA-55, consequently leading to the negative imbalance at TOA. The large negative imbalance at TOA in JRA-55 is not tenable because it implies a cooling of the planet that clearly has not occurred (Trenberth et al., 2011).

Figure 2 is the same as Fig. 1, but at the surface. At surface, all energy fluxes except latent heat flux are within the uncertainty ranges of Wild2014. JRA-55 has a negative energy imbalance over the ocean, whereas the three other reanalyses have a positive imbalance. This may be because the surface latent heat flux in JRA-55 is larger than the estimation of Wild2014 over the ocean. On the contrary, smaller surface latent heat flux appears over the ocean in MERRA, leading to a larger positive global imbalance compared to the other estimations.

The energy imbalances in the four reanalyses that are shown in Fig. 3 are similar to Figs. 1c and 2e except for the 35-year base period of 1979-2013, to confirm the variation of components. The imbalances of the four reanalyses at TOA are increased compared to Fig. 1c, especially in MERRA and CFSR. Compared to Fig. 2e, the surface energy imbalances for reanalyses are also increased by about 0.9-1.7  $W m^{-2}$  over the globe. This means that the average imbalances of the four reanalyses are sensitive to the calibration period because their



**Fig. 4.** Annual mean longwave cloud effect (obtained from the flux difference between TOA-all-sky and TOA-clear-sky) discrepancies between CERES-EBAF data and (a) JRA-55, (b) ERA-Interim, (c) MERRA and (d) CFSR. Positive results indicate that the reanalysis longwave cloud effect is weaker than CERES-EBAF. The global area average and pattern correlation coefficient of each map are included in the upper right and center.



**Fig. 5.** Annual mean surface latent heat flux ( $W m^{-2}$ ) differences between OAF flux data and (a) JRA-55, (b) ERA-Interim, (c) MERRA and (d) CFSR. Positive flux is directed upward. The global area average and pattern correlation coefficient of each map are included in the upper right and center.

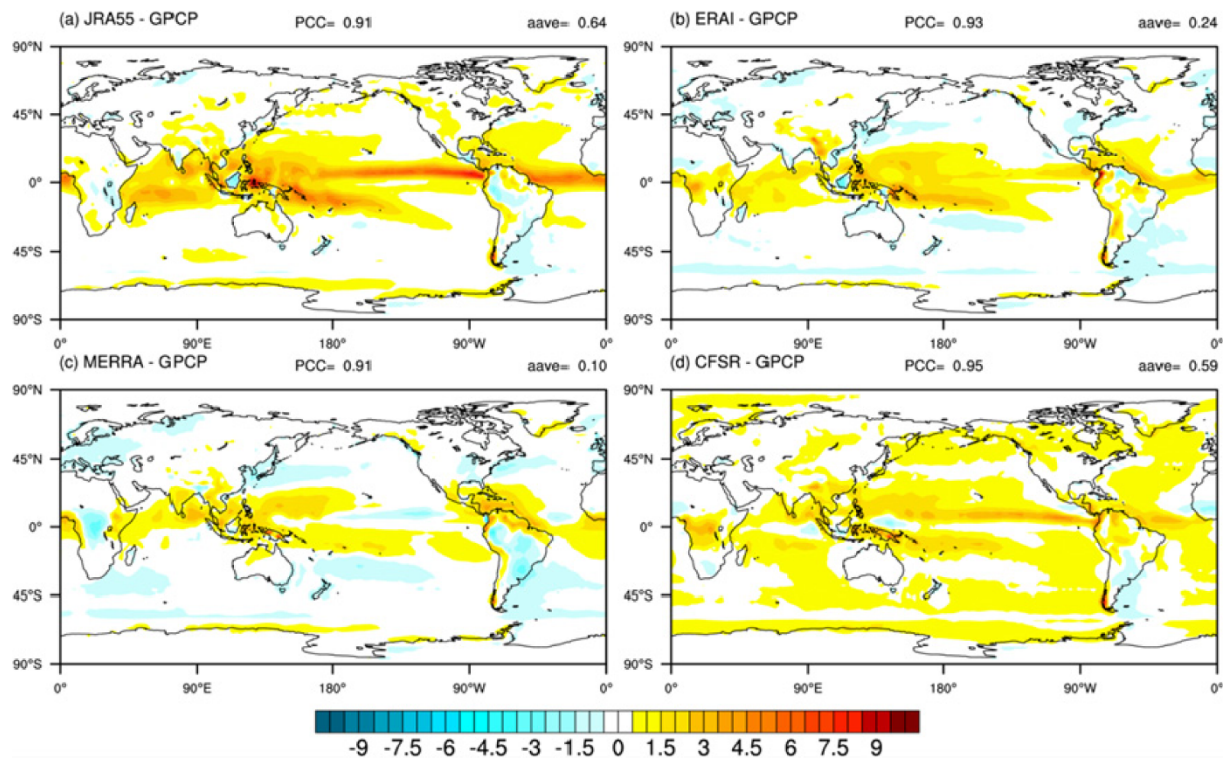


**Fig. 6.** Annual mean precipitation ( $mm d^{-1}$ ) differences for (a) JRA-55, (b) ERA-Interim, (c) MERRA and (d) CFSR, showing differences from GPCP. The global area average and pattern correlation coefficient of each map are included in the upper right and center.

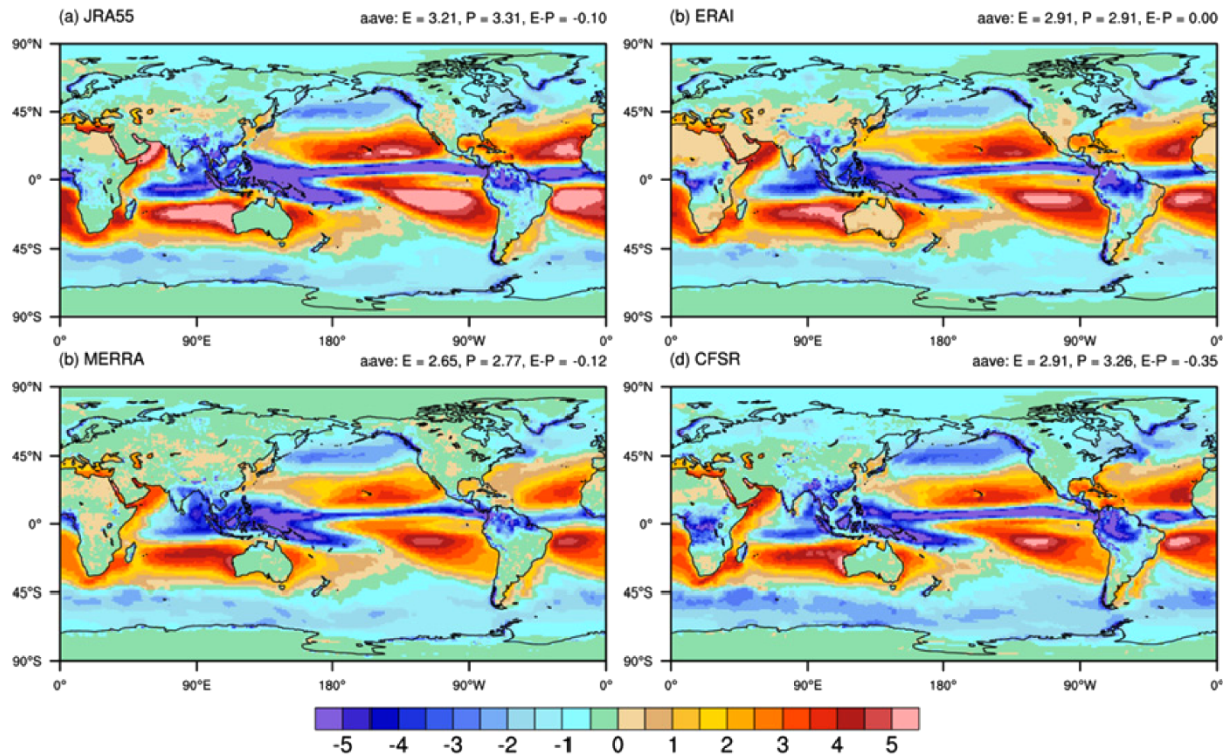


**Fig. 7.** Annual mean E-P ( $\text{mm d}^{-1}$ ) from (a) JRA-55, (b) ERA-Interim, (c) MERRA and (d) CFSR for 2001-2010. The global area average of precipitation, evaporation and E-P are included in the upper right.

energy budgets fluctuate temporally. This demonstrates the need for a study on temporal variations of energy and water budgets. Therefore, the volatility of energy and water components is explored and then discussed in the next section.

The effects of clouds on the energy budget are quantified using cloud radiative forcing defined as the TOA radiative flux differences between clear-sky and all-sky conditions (Charlock and Ramanathan, 1985). Figure 4 compares the TOA longwave cloud effect of JRA-55 and the three other reanalyses with that computed from CERES-EBAF averaged over 2001-2013. The longwave cloud effect is obtained from the flux difference between TOA-all-sky and TOA-clear-sky. Positive values indicate that the longwave cloud effect is weaker than CERES-EBAF. JRA-55 has a generally weaker longwave cloud effect in deep convection regions over the tropics, particularly over the Indian Ocean, the western Pacific, the Intertropical Convergence Zone (ITCZ) and the South Pacific Convergence Zone (SPCZ), compared to CERES-EBAF. These weak longwave cloud effects in JRA-55 lead to excessive OLR, which in turn causes negative net energy flux at TOA (Fig. 1c). The biases in the longwave cloud effects are related to the representation of clouds and the cloud overlap assumptions made in the reanalysis system (Kobayashi et al., 2015).

A distinctive feature of JRA-55 in Fig. 2 is the surface latent heat flux, especially over the ocean, when compared with the three other reanalyses. While latent heat fluxes in ERA-Interim, MERRA and CFSR are closer to or smaller than the

estimation of Wild2014 on a global basis, that in JRA-55 is larger. Figure 5 shows ocean-only difference fields of surface latent heat flux between the four reanalyses and the OAFflux dataset. JRA-55 shows a larger latent heat flux over almost the entire ocean, particularly over the subtropical regions, compared to OAFflux. It may have acted to increase the atmospheric moisture content, with a potentially positive impact on tropical precipitation (Fig. 6).

The differences in precipitation between the four reanalyses and GPCP are illustrated in Fig. 6. The four reanalyses reasonably reproduce the observational patterns. Pattern correlation coefficients (PCCs) are 0.91, 0.92, 0.91, and 0.95 for JRA-55, ERA-Interim, MERRA and CFSR, respectively. Precipitations in middle- and high-latitude regions above  $30^\circ$  are underestimated in MERRA and ERA-Interim, and overestimated in CFSR. In JRA-55, precipitation over the region is in good agreement with observation, although the bias is slightly reduced. On the other hand, JRA-55 overestimates precipitation in the tropics compared with GPCP, especially in ITCZ, SPCZ, Indian Ocean and Atlantic Oceans as in case of latent heat flux. Kobayashi et al. (2015) attributed such bias mostly to large moistening increments and the spin-down problem of reanalysis system, which immediately causes excessive precipitation after the start of forecasts.

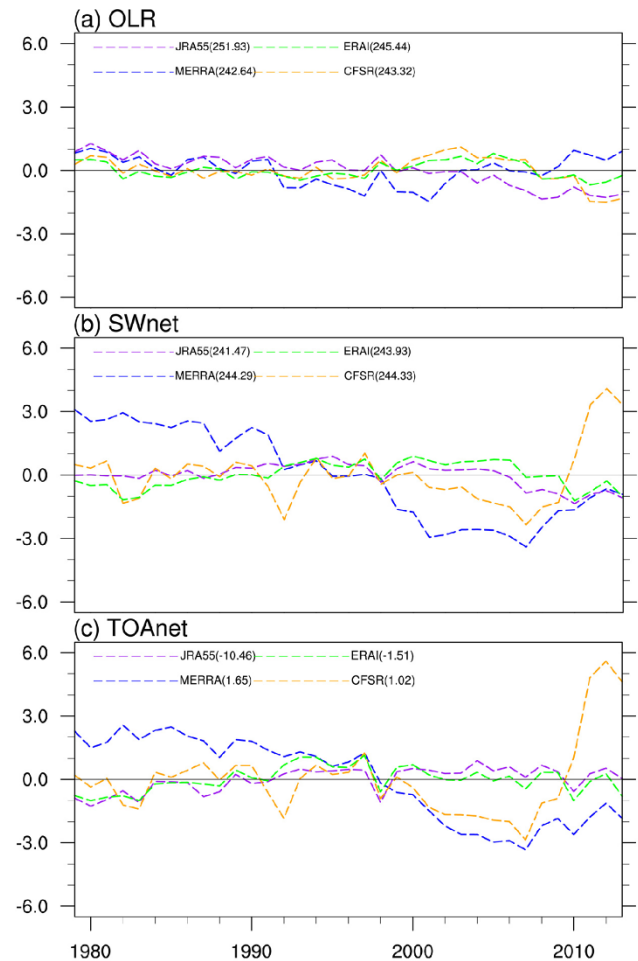
The difference between evaporation and precipitation (E-P) is an integral parameter of the global water balance. E-P results from the four reanalyses during 2001-2013 are shown in Fig.

7. All reanalyses show similar patterns over the ocean, with relatively negative E-P over ITCZ, SPCZ and regions of the ocean basins that are related to storm track activity, and relatively positive E-P in the trade-wind regimes in the eastern parts of the oceans. JRA-55 has strong negative E-P over ITCZ and SPCZ because of the overestimated precipitation, but strong positive E-P over extratropical regions due to the overestimated evaporation. In general, E-P is negative over land, but all reanalyses show several areas that potentially violate this physical constraint. Especially, the value for E-P is positive in ERA-Interim over Australia but is not in the three other reanalyses. The positive value for MERRA over the Southern African monsoon region was ascribed by Bosilovich et al. (2011) to an erroneous radiosonde station. Such positive areas also appear in JRA-55 and CFSR although to a lesser extent. To analyze the components contributing to the global water balance, the global area average of precipitation, evaporation and E-P are separately calculated and presented in Fig. 7. ERA-Interim shows a reasonable closure of the global water balance, although the water budget is unrealistic over land. The global water balances are also close to zero in JRA-55 and MERRA, but each component of those is different to that of ERA-Interim. In other words, JRA-55 generally overestimates both precipitation and evaporation, while MERRA slightly underestimates them.

### b. Interannual variability

As aforementioned, we examine the temporal variability of reanalyses to confirm actual changes in the components of the global energy and water balances. Variations of the observing system in the reanalysis data assimilation can cause spurious variations in the reanalysis time series (Saha et al., 2010; Bosilovich et al., 2011; Dee et al., 2011). For instance, MERRA and CFSR show the strongest shifts in water and energy budgets which coincide with the availability of Advanced Microwave Sounding Unit-A (AMSU-A) instruments (Saha et al., 2010; Bosilovich et al., 2011).

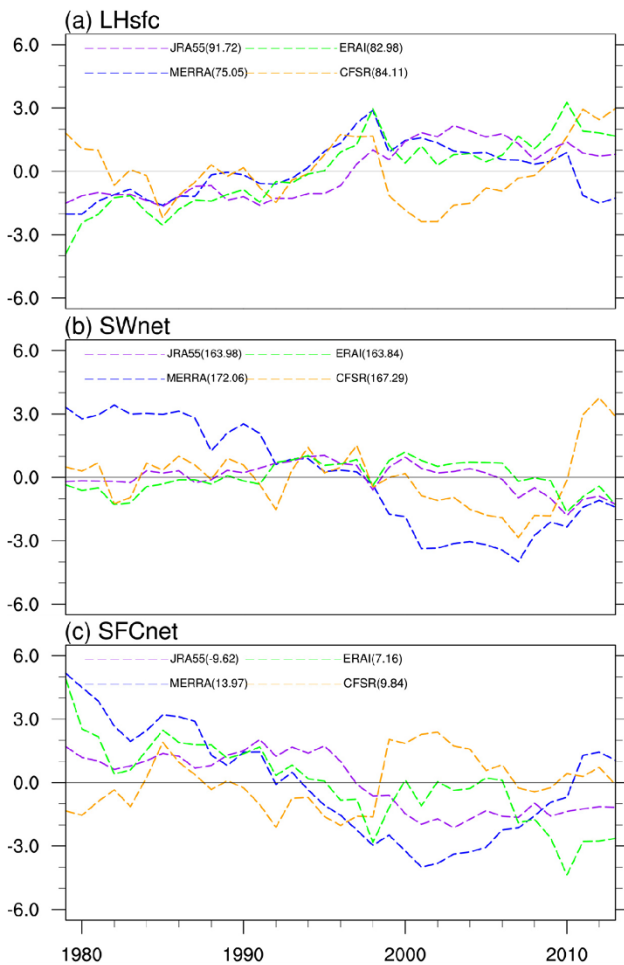
Figure 8 shows the time series of global annual anomalies for OLR, net shortwave radiation (the difference between downward shortwave radiation and upward shortwave radiation) and energy budget at TOA. In all reanalyses, the variation of OLR is much smaller than those of net shortwave radiation and the global energy budget. The time series of global energy budget is highly correlated with global net shortwave radiation. Net shortwave radiation and energy budget show a strong interannual variability in MERRA and CFSR, while JRA-55 and ERA-Interim exhibit less trends and remain stable. The time series of global annual anomalies for latent heat flux, net shortwave radiation and energy budget at surface are shown in Fig. 9. The interannual variability of energy budget at the surface highly correlates with latent heat flux in JRA-55, CFSR and ERA-Interim, while the energy budget of MERRA has very similar variability to that of net shortwave radiation. JRA-55 shows a slightly increasing trend



**Fig. 8.** Global annual anomalies from JRA-55, ERA-Interim, MERRA and CFSR for (a) OLR, (b) net shortwave radiation at TOA (SWnet) and (c) net top of atmosphere radiation (TOAnet). The global area averages of those are included in the legend. Units are  $\text{W m}^{-2}$ .

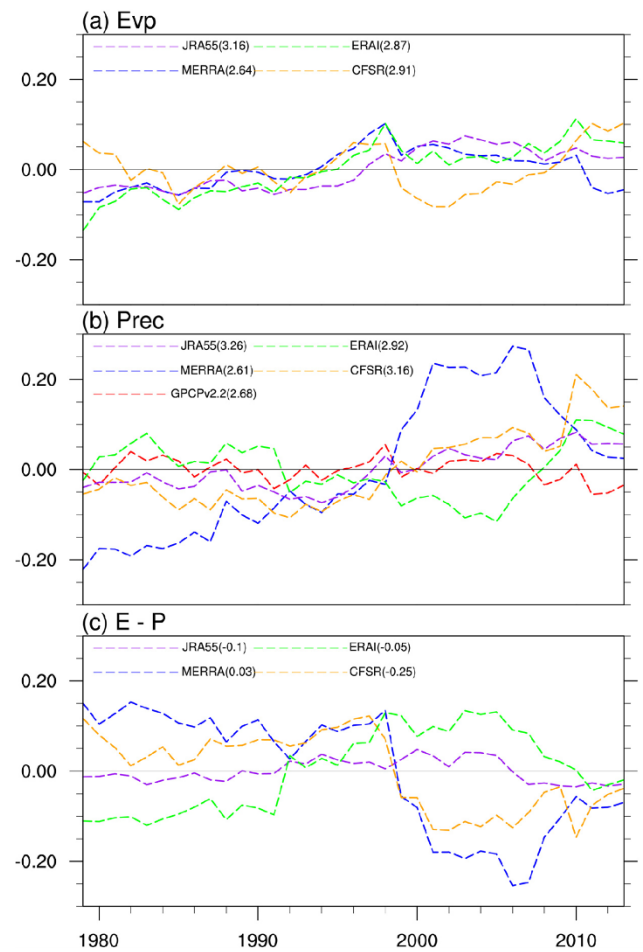
in the latent heat flux, which decreases the net energy budget. In MERRA, major stepwise changes occur in net shortwave radiation at TOA and surface, most notably in the precipitation (Fig. 10b).

Figure 10 shows the time series of global annual anomalies of precipitation, evaporation and E-P. The GPCP v2.2 annual anomaly is shown in Fig. 10b, together with reanalyses for comparison. Aside from JRA-55, significant stepwise changes of precipitation occur in MERRA, CFSR and ERA-Interim, which is not seen in GPCP. These changes are clearly shown in E-P. Between 1998 and 2001, MERRA shows strong E-P downward shifts affected only by precipitation. These are caused by the addition of new AMSU-A instrumentations on NOAA-15(1998) and NOAA-16(2001) (Bosilovich et al., 2011). CFSR also shows strong E-P downward shifts, but these are affected by increased precipitation and decreased evaporation. Saha et al. (2010) note that the significant decrease (increase) in evaporation (precipitation) around 1998~2001 is related to AMSU-A. Contrary to MERRA and CFSR, ERA-Interim exhibits an upward E-P shift in 1992 affected by



**Fig. 9.** Same as in Fig. 8, but for (a) surface latent heat flux, (b) net shortwave radiation at surface and (c) net surface energy flux.

decreased precipitation due to changes in observations from the Special Sensor Microwave/Imager (SSM/I) of new Defense Meteorological Satellite Program (DMSP) satellites. Precipitation in ERA-interim decreases from 1992 to 2005, which is entirely explained by a problem in the 1D+4D-Var rain assimilation scheme, which depends on the number of SSM/I observations. Since 2006, the trend in this precipitation anomaly becomes gradually increasing due to the decreased number of observations in 2006 (Dee et al., 2011). JRA-55 exhibits reasonable stability and less trends. According to the previous study (Trenberth and Smith, 2008; Trenberth et al., 2011), JRA-25 also shows a large and abrupt drop in the hydrological cycle in mid-1987, which coincides with the start of the assimilation of SSM/I and upward drift in 1998 related to AMSU-A. As noted by Kobayashi et al. (2015), the increments of specific humidity on assimilation in JRA-55 do not exhibit the impacts of changes in observing systems as clearly as do those in JRA-25. Therefore, JRA-55 reduced the basic problem of creating a long-term homogeneous product (Thorne and Vose, 2010), and consequently affords more time-consistent retrospective analysis.



**Fig. 10.** Same as in Fig. 8, but for (a) evaporation from the reanalyses, (b) precipitation from the reanalyses and GPCP v.2.2 and (c) E-P from the reanalyses.

#### 4. Summary and discussion

In this study, JRA-55 is evaluated in comparison with three other recent reanalyses, namely, ERA-interim, MERRA and CFSR, in light of global energy and water balances. First, global climate energy balances in the four reanalyses were compared with previous estimations (Wild et al., 2014) and observations. JRA-55 has larger OLR and surface latent heat flux, leading to negative net energy fluxes at TOA and surface, respectively. JRA-55 clouds are optically weaker than those of the three other reanalyses, leading to excessive OLR, which in turn causes negative net energy flux at TOA. At the surface, JRA-55 also has a negative imbalance, which can be accounted for by systematic positive biases in the surface latent heat flux over the ocean. The global water balance was investigated in terms of global mean E-P distribution. All reanalyses show similar E-P spatial patterns. JRA-55 has a relatively strong negative (positive) E-P in ITCZ and SPCZ (extratropical regions) due to overestimated precipitation (evaporation). Over land, ERA-Interim shows several positive E-P areas which are generally not present. Such positive areas also appear in JRA-

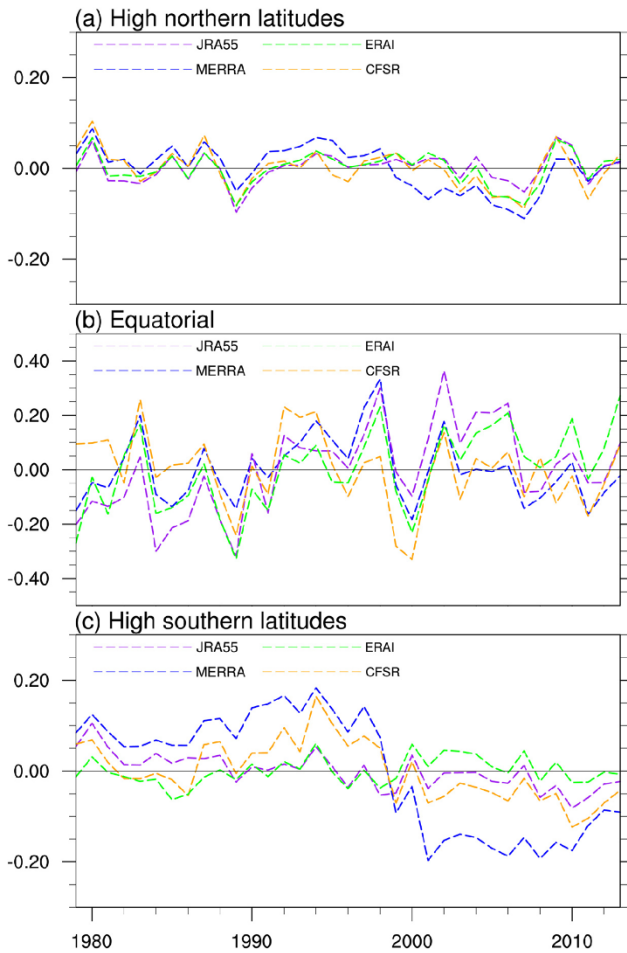


**Fig. 11.** Annual E-P anomalies from JRA-55, ERA-Interim, MERRA and CFSR averaged over high northern latitudes (a), Equatorial (b), and high southern latitudes (c). Units are  $\text{mm d}^{-1}$ .

55 and CFSR, although to a lesser extent.

In the analysis of annual time series, all reanalyses show that the interannual variation in net radiative energy follows that of the net shortwave radiation at TOA. JRA-55 and ERA-interim exhibit less trends and remain stable compared to MERRA and CFSR. At surface, the energy budgets of JRA-55, CFSR and ERA-Interim are affected by the latent heat flux much more than by net shortwave radiation. However, MERRA is more affected by net shortwave radiation. In E-P time series, significant stepwise changes occur in MERRA, CFSR and ERA-Interim due to the changes in the observing system used in data assimilation. A strong E-P downward shift occurs in MERRA and CFSR around 1998 due to the addition of new AMSU-A. ERA-Interim exhibits an E-P upward shift in 1992 due to changes in observations from SSM/I of new DMSP satellites. Unlike the three other reanalyses, however, JRA-55 exhibits less trends and remains more stable without unnatural changes throughout the reanalysis period.

The causes for the contrasting E-P change around the 1990s in JRA-55 compared to CFSR, MERRA and ERA-Interim are

more difficult to interpret. The discrepancy may be explained by a difference in the use of satellite radiances and improved data assimilation system. The computing algorithm for total column cloud water retrievals from AMSU-A has been updated since JRA-25 (Kobayashi et al., 2015) because the problem was already found in JRA-25 (Onogi et al., 2007). The shift in precipitation in ERA-interim is caused by a problem in the 1D+4D-Var rain assimilation scheme (Dee et al., 2011). The rain assimilation scheme may have been improved in the JRA-55 system.

Regional perspectives on the energy and water balance are important as well as globe. In order to briefly explore regional variability, we additionally investigated E-P time series by diving into equatorial, the high northern and southern latitudes. Figure 11 presents annual E-P anomalies from JRA-55, ERA-Interim, MERRA and CFSR averaged over high northern latitudes ( $60^{\circ}\text{N}\sim$ ), Equatorial ( $20^{\circ}\text{S}\sim 20^{\circ}\text{N}$ ), and high southern latitudes ( $\sim 60^{\circ}\text{S}$ ). According to the result, the E-P shift shown in globe also appears in the high southern latitudes. Nicolas and Bromwich (2011) has demonstrated that the observational constraint is still largely absent over the high southern latitudes, leading to artificial trends and jumps in reanalysis time series. Therefore, inconsistency of energy and water shows different behaviors between regions because it may be highly correlated with spatial variation of observation's quality and dense. More insights into regional energy and water balance are needed.

Global reanalysis datasets are produced via data assimilation system and numerical model which ingest all available observational data. It is difficult to estimate natural variability using reanalysis datasets, because climate variations and trends are seriously affected by historical changes of observational data, especially satellite data. Trenberth and Smith (2008) also pointed out lower accuracy of variability on multi-year timescales in the present reanalysis. But recently, JRA has been trying to improve the accuracy of variability in the reanalysis by controlling observational data. In details, JRA has started to produce a reanalysis assimilating conventional observations only, called JRA-55C. We believe that comparison between JRA-55 and JRA-55C will help to estimate the natural variability as well as numerical model bias in reanalysis datasets.

**Acknowledgments.** This work was carried out with the support of the Korea Meteorological Administration Research and Development Program under grant KMIPA 2015-2081 and the Rural Development Administration Cooperative Research Program for Agriculture Science and Technology Development under Project No. PJ009353, Republic of Korea.

**Edited by:** John McGregor

## REFERENCES

- Adler, R. F., and Coauthors, 2003: The Version-2 Global Precipitation Climatology Project (GPCP) monthly precipitation analysis (1979-present), *J. Hydrometeorol.*, **4**, 1147-1167, doi: 10.1175/1525-7541(2003)

- 004<1147:TVGPCP>2.0.CO;2.
- Bosilovich, M. G., F. R. Robertson, and J. U. Chen, 2011: Global energy and water budgets in MERRA. *J. Climate*, **24**, 5721-5739, doi:10.1175/2011JCLI4175.1.
- Charlock, T. P., and V. Ramanathan, 1985: The albedo field and cloud radiative forcing produced by a general circulation model with internally generated cloud optics. *J. Atmos. Sci.*, **42**, 1408-1429.
- Cullather, R. I., and M. G. Bosilovich, 2012: The energy budget of the polar atmosphere in MERRA. *J. Climate*, **25**, 5-24, doi: 10.1175/2011-JCLI4138.1.
- Dee, D. P., and Coauthors, 2011: The ERA-Interim reanalysis: configuration and performance of the data assimilation system, *Quart. J. Roy. Meteor. Soc.*, **137**, 553-597, doi: 10.1002/qj.828.
- Ebita, A., and Coauthors, 2011: The Japanese 55-year reanalysis "JRA-55": an interim report. *Sci. Online Lett. Atmos.*, **7**, 149-152, doi: 10.2151/sola.2011-038.
- Hodges, K. I., R. W. Lee, L. Bengtsson, 2011: A comparison of extratropical cyclones in recent reanalyses ERA-Interim, NASA MERRA, NCEP CFSR, and JRA-25, *J. Climate*, **24**, 4888-4906, doi: 10.1175/2011JCLI4097.1.
- Kobayashi, S., and Coauthors, 2015: The JRA-55 Reanalysis: General specifications and basic characteristics, *J. Meteor. Soc. Japan.*, **93**, 5-48, doi: 10.2151/jmsj.2015-001.
- Loeb, N. G., B. A. Wielicki, D. R. Doelling, G. L. Smith, D. F. Keyes, S. Kato, N. Manalo-Smith, and T. Wong, 2009: Toward optimal closure of the earth's top-of-atmosphere radiation budget. *J. Climate*, **22**, 748-766, doi: 10.1175/2008JCLI2637.1.
- Nicolas, J. P., and D. H. Bromwich, 2011: Precipitation changes in high southern latitudes from global reanalyses: a Cautionary Tale. *Surv. Geophys.*, **32**, 475-494, doi: 10.1007/s10712-011-9114-6
- Onogi, K., and Coauthors, 2007: The JRA-25 reanalysis. *J. Meteor. Soc. Japan*, **85**, 369-432, doi: 10.2151/jmsj.85.369.
- Quadro, M. F. L., E. H. Berbery, M. A. F. S. Dias, D. L. Herdies, and L. G. G. Gonçalves, 2013: The atmospheric water cycle over south America as seen in the new generation of global reanalyses, *AIP Conf. Proc.*, **1531**, 732-735, doi: 10.1063/1.4804874.
- Rienecker, M. M., and Coauthors, 2008: The GEOS-5 Data Assimilation System Documentation of Versions 5.0.1, 5.1.0 and 5.2.0. Tech. Rep. Series on Global Modeling and Data Assimilation, M. J. Suarez, Ed., NASA/TM-2008-104606, Vol. 27, National Aeronautics and Space Administration Goddard Space Flight Center, 95 pp.
- \_\_\_\_\_, and \_\_\_\_\_, 2011: MERRA: NASA's modern-era retrospective analysis for research and applications, *J. Climate*, **24**, 3624-3648, doi: 10.1175/JCLI-D-11-00015.1.
- Saha S., and Coauthors, 2010: The NCEP climate forecast system reanalysis, *Bull. Amer. Meteor. Soc.*, **91**, 1015-1057, doi: 10.1175/2010-BAMS3001.1.
- Stephens, G. L., J. Li, M. Wild, C. A. Clayson, N. Loeb, S. Kato, T. L'Ecuyer, P. W. Stackhouse Jr, M. Lebsock, and T. Andrews, 2012: An update on Earth's energy balance in light of the latest global observations, *Nature Geoscience*, **5**, 691-696, doi:10.1038/ngeo1580.
- Thorne, P. W., and R. S. Vose, 2010: Reanalysis suitable for characterizing long-term trends: Are they really achievable? *Bull. Amer. Meteor. Soc.*, **91**, 353-361, doi:10.1175/2009BAMS2858.1.
- Trenberth, K. E., and L. Smith, 2008: Atmospheric energy budgets in the Japanese reanalysis: evaluation and variability. *J. Meteor. Soc. Japan*, **86**, 579-592, doi: 10.2151/jmsj.86.579.
- \_\_\_\_\_, J. T. Fasullo, and J. Kiehl, 2009: Earth's global energy budget, *Bull. Amer. Meteor. Soc.*, **90**, 311-323, doi: 10.1175/2008BAMS2634.1.
- \_\_\_\_\_, and \_\_\_\_\_, 2010: Simulation of present-day and twenty-first-century energy budgets of the Southern Oceans, *J. Climate*, **23**, 440-454, doi: 10.1175/2009JCLI3152.1.
- \_\_\_\_\_, \_\_\_\_\_, and J. Mackaro, 2011: Atmospheric moisture transports from ocean to land and global energy flows in reanalyses, *J. Climate*, **24**, 4907-4924, doi: 10.1175/2011JCLI4171.1.
- Uppala, S., D. Dee, S. Kobayashi, P. Berrisford, and A. Simmons, 2008: Towards a climate data assimilation system: status update of ERA-Interim. ECMWF Newsletter, **115**, 12-18 pp. [Available at <http://old.ecmwf.int/publications/newsletters/pdf/115.pdf>].
- Wild, M., D. Folini, M. Z. Hakuba, C. Schär, S. I. Seneviratne, S. Kato, D. Rutan, C. Ammann, E. F. Wood, and G. König-Langlo, 2014: The energy balance over land and oceans: an assessment based on direct observations and CMIP5 climate models. *Clim. Dyn.*, **44**, 3393-3429, doi: 10.1007/s00382-014-2430-z.
- Yu, L., and R. A. Weller, 2007: Objectively analyzed air-sea heat fluxes for the global ice-free oceans (1981-2005). *Bull. Amer. Meteor. Soc.*, **88**, 527-539, doi: 10.1175/BAMS-88-4-527.